

Macquarie University ResearchOnline

This is the published version of:

Saghafi, S., Withford, M., Latifi, H. & Piper, J. A., "Beam propagation analysis in unstable laser resonators (ULR) : low to high magnification," Proceedings of SPIE, 4829, 8-9, (2003).

Access to the published version:

<http://dx.doi.org/10.1117/12.523670>

Copyright:

Copyright 2003 Society of Photo Optical Instrumentation Engineers. One print or electronic copy may be made for personal use only. Systematic reproduction and distribution, duplication of any material in this paper for a fee or for commercial purposes, or modification of the content of the paper are prohibited.

Beam propagation analysis in unstable laser resonators (ULR); low to high magnification

#*Saiedeh Saghafi, *Michael Withford, #H. Latifi and *James A. Piper
Laser Research Institute, Shahid-Beheshti University, Tehran, Iran

*Physics Department, Macquarie University, Sydney, NSW 2109, Australia
ssaghafi@sbu.cc.ac.ir, Tel: (+9821) 2990 2696, Fax: (+9821) 241 8698

ABSTRACT

Lasers employing unstable resonators usually produce a doughnut-shaped intensity distribution in the near-field. In this paper, we present the application of a new model in characterising the output beams of unstable laser resonators (ULR) of different magnification ($M=80, 200, \text{ and } 400$). As an experimental example, the output beam of Copper Vapour Laser (CVL) is characterised using this model.

INTRODUCTION

Generally, the usefulness of a model is established from how well it can predict what is observed experimentally. Based on the Flattened Gaussian Beams (FGBs) model [1], a new analytical expression called the Flattened Gaussian Beams with a Hole in the Middle (FGBHM) was introduced by Saghafi et. al.[2]. By changing a variable constant called η , various beam profiles can be developed and by using the propagating formula, at different transverse planes, the intensity profile at any arbitrary plane can be predicted.

One type of high power laser employing unstable resonators is the CVL that is described as a multi-pass amplifier of an initial burst of seed radiation. It has been shown that the beam quality of CVL output can be significantly improved by employing high magnification unstable resonators. Magnification is the ratio of the high reflector's radius of curvature to the spot reflector's radius of curvature. In this paper, the FGBHM model is employed to characterise the output beam of ULR of $M=80, 200, \text{ and } 400$.

THE FGBHM

Gori introduced a new type of axially symmetric beams, termed Flattened Gaussian Beams (FGBs) in 1994 [1]. At the waist, the beam is described as a finite sum of Laguerre-Gaussian functions:

$$\psi(r,0) = A \sum_{n=0}^N C_n L_n \left(\frac{2Nr^2}{w_0^2} \right) \exp \left[-\frac{N}{w_0^2} r^2 \right], \quad N=1, 2, 3, \dots \quad (1)$$

where A, w_0, L_n , and N are as given in ref.[1]. The superposition of a standard FGB model, as described by Eq.1, with an *additional* FGB (called the constructed FGB), creates a central shadow and gives an expression for a Flattened Gaussian Beam with a Hole in the Middle (FGBHM) [2]. In the near-field when $z=0$, the constructed FGB for which the amplitude distribution and steepness can be varied from that of Eq.1, is written as:

$$\psi_B(r,0) = A \sum_{n=0}^B C_n^B L_n \left(\frac{2Br^2}{v_0^2} \right) \exp \left[-\frac{Br^2}{v_0^2} \right], \quad B = 1, 2, 3, \dots \quad (2)$$

where C_n^M , the spot size, and other related parameters of this beam was given in ref.[2]. The superposition of these two FGBs along the z -axis is thus:

$$\psi_w(r,z) = \psi_N(r,z) + \eta \psi_B(r,z), \quad (3)$$

where M , the beam order of the constructed FGB, controls the steepness of the shoulders of the hole, and η is a variable constant which enables various spatial intensity distributions to be achieved [2].

OUTPUT BEAM ANALYSIS OF ULR FOR $M=80, 200, \text{ AND } 400$

The optical resonator for these experiments consisted of a negative branch on-axis unstable, confocal resonator formed by a $R_1 = 4m$ high reflector (50mm diameter) at one end, with 1mm diameter scraper mirror (i.e. 1 mm axial elliptical mirror located on a 50mm clear optical element) directing the centre of the beam onto an auxillary reflector at the other end. The diameter of the on-axis shadow is 1mm. Note that the small size of this shadow increases diffraction effects extend and the wings of the intensity distribution thereby causing a larger beam width in the far-field study. In this study, to produce beams with different beam quality, the high reflector had a fixed radius of curvature of 4 m whereas the radius of curvature of the auxillary reflector varied from 1 cm, 2 cm, and 5 cm to create $M=400, 200, \text{ and } 80$ respectively. As M decreases additional low quality components appears in the output beam and provide a useful test for the FGBHM model over a range of conditions ($M=400, 200 \text{ and } M=80$). In each case the beam was collimated, using a collimator tester by adjusting the distance between R_2 and the scraper mirror. It must be noted that, at $z=0$ (the

first plane of measurement), the differences between the output intensity profiles for three magnifications are negligible (Fig.1) and their differences are more pronounced at far-field.

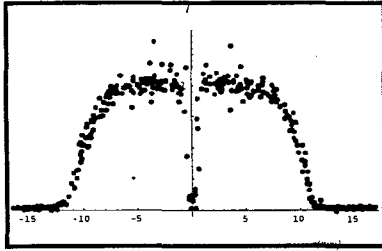


Fig.1 The intensity profiles for M=400, 200, 80 ($z=0$)

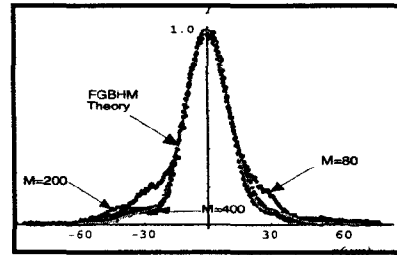


Fig.2 The intensity profiles for M=400, 200, 80 (far-field)

The far-field distributions in these three cases share a dominant central peak. For M=400 the wings approximate an Airy disk distribution, however, for the M=200 resonator the wings on either side become larger, indicating larger contributions from the more divergent components. This effect is more pronounced for the M=80 case where these wings are washed out giving the impression of a larger beam diameter. Furthermore, due to clipping by the aperture (front of laser cavity), the divergence angle in all cases becomes larger than the one predicted by the paraxial approximation. Consequently, the beam width predicted by theory is smaller than the real one (due to the smaller angle of divergence) and theory can produce a beam profile similar to the experimentally measured one by replacing z with a constructed z_T . This constructed z_T can be determined by the angle of divergence [2]. Using our measurements in the near- and far-field, M^2 and thus, the angle of divergence can be calculated. In the near-field the differences between the output intensity profiles for three magnifications are negligible (Fig.1), so a similar kurtosis factor for three cases in the near-field ($z=0$) can be estimated. Using the measured data at $z=0$, k is defined as 1.829. The beam order using the kurtosis factor can be defined as $N = 30 \pm 1$ using Eq.4.

$$N = \sqrt{\frac{1.54}{(k-1.8)^2} - \sqrt{k-1.8} + (k-1.8)} \quad (4)$$

RESULTS AND DISCUSSION

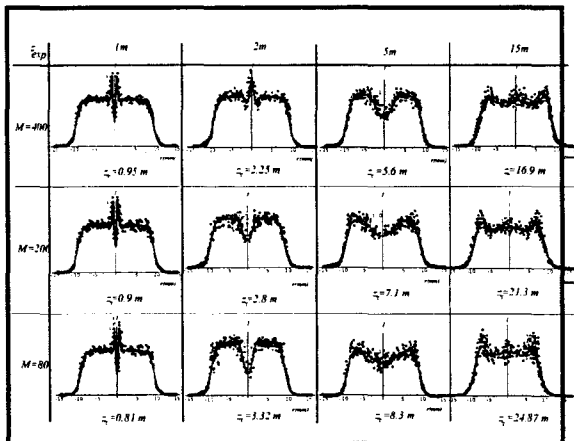


Fig.3 The intensity profiles for M=400, 200, 80 ($z=1, 2, 5, \text{ and } 15m$)

Comparisons between the beam intensity profiles in the near-field, with the theoretical distribution at $z=1, 2, 5, 15m$, are illustrated in Fig.3. It has been shown in these figures that at $z \sim 1m$, the differences between the output intensity profiles for three cases are not significant. At $z=2m$, the differences between the beam intensity profiles produced by ULRs having different magnifications begin to show. For the M=400 case, the constructed and experimental z are very close, at $z=2m$,

a central peak is appeared. For both the M=200 and 80 cases a central trough appears at $z=2m$. However, for M=200 the depth of the central trough is less than the M=80 case. At $z=5m$, the intensity profiles of the three conditions have similar distributions (a central trough and two peaks), however, for M=400 the two peaks are flatter than the other cases and the degree of flatness decreases from M=200 to M=80. Similarly at $z=15m$, the shoulders of the intensity distributions of these unstable resonators lose their flatness entirely and become sharp. The central trough indicated at $z=5m$ is replaced by a small peak.

It can be seen that by measuring the beam intensity profiles at two planes of measurement ($z=0$, and far-field), we are able to estimate the beam parameters (M^2 and k), the model parameters (beam order), angle of divergence and the constructed z . Using these factors, the beam intensity profiles at any arbitrary point can be predicted.

REFERENCE

1. F. Gori, Opt.Com., **107**, pp. 335-341, 1994.
2. S. Saghaei M. J, Withford., and J. A Piper., J. Opt. Soc. Am. A: Special edition on Free and Guided Beams, **18**, 1, (2001).
3. A. E Siegman., Proc. of SPIE, **1224**, 2, (1990).
4. T. F., Jr., Johnston, Laser Focus World, **173**, (May 1990).